Available online at www.sciencedirect.com

ScienceDirect

Procedia Engineering 109 (2015) 80 – 88

Procedia Engineering

www.elsevier.com/locate/procedia

XXIII Italian Group of Fracture Meeting, IGFXXIII

Fatigue behavior of shot peened notched specimens: effect of the residual stress field ahead of the notch root

M. Benedetti[a], V. Fontanari[a,*], B. Winiarski[b], P.J. Withers[b], M. Allahkarami[c], J.C. Hanan[c]

[a]*University of Trento, via Sommarive 9, 38123 Trento, Italy*
[b]*University of Manchester, Grosvenor Street, Manchester, M13 9PL, U.K.*
[c]*Oklahoma State University, 700 N. Greenwood Ave., 74106 Tulsa, OK, U.S.A.*

Abstract

Shot peening strongly increases the notch fatigue strength of metallic components. This benefit is mainly attributed to compressive residual stresses. In this paper, we address this topic by performing bending fatigue tests on Al-7075-T651 samples carrying notches with different severity. Fatigue lives between 10^5 and 10^8 cycles have been explored. The residual stress field ahead of the notch has been characterized by experimental measurements and numerical reconstruction and incorporated into the Crossland fatigue criterion combined with critical distance theory method to predict the fatigue resistance.

Peer-review under responsibility of the Gruppo Italiano Frattura (IGF)

Keywords: Shot peening; notch fatigue; Al-7075-T651; residual stresses; critical distance theory

1. Introduction

Shot peening is a surface treatment consisting of bombarding the metallic surface to be treated with a large number of small spherical hard shots under controlled conditions, thus producing plastic deformation in a shallow surface region and leading to a compressive surface residual stress (RS) state [1]. This treatment is widely applied to improve the fatigue resistance of mechanical components carrying stress raisers or notches, because it can treat, with near-full coverage, geometrical details that are inaccessible to other surface treatment, like hammer or ultrasonic peening or

* Corresponding author. Tel.: +39-0461-282430; fax: +39-0461-281977.
E-mail address: vigilio.fontanari@ing.unitn.it

Peer-review under responsibility of the Gruppo Italiano Frattura (IGF)
doi:10.1016/j.proeng.2015.06.210

ball burnishing. Shot peening mainly results in three fatigue related modifications of the surface layers: roughness, residual stresses and work hardening. The surface roughening is detrimental to the fatigue resistance, but this issue is less felt in notched components owing to the notch shadowing of the stress concentration due to surface dimples. The increment in fatigue strength and reduction in notch fatigue sensitivity given by shot peening is deemed to be strongly correlated to the RSs produced by the treatment [2].

The fatigue behavior of shot peened plain and notched specimens under reverse bending loading conditions (R = -1) was investigated in [3-5], finding a concomitant increment in fatigue strength and reduction in notch sensitivity. In-depth RS profiles were measured on plain samples before and after fatigue tests. The observed RS relaxation was mainly imputed to plastic flow occurring when the superposition of residual and external stresses exceeds the material's cyclic compressive yield strength. Since the experimental determination of RSs near geometrical discontinuities is very difficult, a simplified numerical approach to reconstruct the RS field was adopted. Specifically, eigenstrains determined from RS measurements undertaken on plain specimens were transferred to the frontal surface of notched samples, neglecting the peening contribution on the lateral surface at the notch root as well as boundary effects at the edge between frontal and lateral surfaces. The Sines criterion was considered to incorporate stabilized RSs as mean stresses, combined with a line method based on the critical distance theory to account for the notch sensitivity. Despite the approximate estimation of the initial RS distribution at the notch root, reasonable agreement with the experimental data was found, because under reverse bending, the stabilized RS field at the notch apex is mainly dictated by the maximum compressive RS tolerated by the material in the elastic regime rather than the initial RS field [6].

Recently [7] the multiaxial fatigue behavior of untreated and shot peened high-strength Al alloy was investigated. The Crossland criterion was found to efficiently capture the sensitivity of Al-alloys to the RS field and mean external stresses. In [8] the very high-cycle fatigue resistance of variously shot peened Al-alloys under pulsating bending loading was studied, finding that the shot peening effect on the very-high cycle fatigue behavior cannot be explained solely by a multiaxial (crack initiation) fatigue criterion, since a complex interaction between non-propagating surface cracks and sub-superficial cracks was found.

The present paper is aimed at investigating the high and very-high-cycle fatigue behavior of shot peened notched specimens. For this purpose, pulsating bending fatigue tests (R = 0.05) have been carried out on smooth and notched samples exploring fatigue lives comprised between 10^5 and 10^8 cycles. The RS field ahead of the notch root has been carefully evaluated, using non-destructive and destructive techniques, namely micro-XRD (μXRD) and FIB-DIC micro-slot cutting (μSC) and micro-hole drilling (μHD) to map RSs along the notch bisector. These measurements are used to reconstruct the RS field through finite element (FE) analyses. The fatigue results are interpreted on the basis of the Crossland criterion incorporating the reconstructed RSs as mean stresses. Notch sensitivity is accounted for by averaging the stress field over a material characteristic length according to the theory of critical distance.

2. Materials and experimental procedures

The experimentation is performed on Al-7075-T651 alloy supplied in the form of 4 mm thick rolled plate. The monotonic tensile and the fatigue tests carried out on plain specimens according to ISO 3928 can be found in [3] and [8] respectively. The smooth and notched specimens are extracted from the plate with the stress axis parallel to the L-direction of the microstructure. The notched specimens, whose geometry is illustrated in Fig. 1, were accurately manufactured by Electric Discharge Machining (EDM) producing fillet radius r of 2 mm (''blunt" notch), 0.5 mm (''sharp" notch) and 0.15 mm (''very sharp" notch), having theoretical stress concentration factor of 1.5, 2.3 and 3.7, respectively.

Controlled shot peening on all specimens sides, including notch root, was performed. Details about the process and the air-blast machine can be found in Ref. [3]. The treatment employs small ceramic beads leading to a gentle and superficial effect, allowing for better coverage of small geometrical details and higher fatigue performance as compared with larger shots.

Pulsating (R = 0.05) load-controlled 4-point bending fatigue tests are carried out in air, at room temperature, and at a nominal frequency of 110 Hz using a resonant testing machine Rumul Mikrotron 20 kN equipped with a 1 kN load cell. Different stress levels corresponding to fatigue lives in the range between nearly 10^5 and 10^8 cycles are considered. Tests are terminated at 10^8 cycles when no fracture occurs.

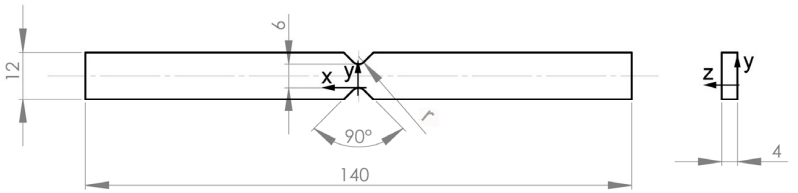

Specimen	r (mm)
Blunt notched	2
Sharp notched	0.5
Very sharp notched	0.15

Fig. 1. Geometry of notched specimens used in this study. All dimensions are given in mm.

Two types of fatigue curves are obtained, i.e. without and with knee located around 10^6 fatigue cycles. The former fatigue curves, corresponding to 50% of failure probability, are represented by a S-N curve in the form of:

$$\sigma_{P50} = \sigma_{0P50} \times N_f^{-\frac{1}{k}} \tag{1a}$$

The latter fatigue curves, corresponding to 50% of failure probability, are represented by a S-N curve in the form of:

$$\sigma_{P50} = \sigma_{0P50} + \frac{k}{N_f} \tag{1b}$$

It should be noted that the meaning of the coefficients of Eqs. (1a-b) is different, but they have been taken the same for a concise presentation in Table 3. In both cases, the uncertainty range is assumed to be constant and approximated by its centroid value. As a representative value of the scatter, the following expression is used:

$$T\sigma = 1 : \sigma_{P90} / \sigma_{P10} \tag{2}$$

P_{90}, P_{10} denote the 90% and 10% levels of failure probability, respectively. The notch sensitivity factor q at a given number of cycles to failure N_f is computed as:

$$q\left(N_f\right) = \frac{K_f\left(N_f\right) - 1}{K_t - 1}; \quad K_f\left(N_f\right) = \frac{\sigma_{P50,smooth}\left(N_f\right)}{\sigma_{P50,notched}\left(N_f\right)} \tag{3}$$

The modifications of the surface layers produced by shot peening were investigated in [9] through surface roughness and in-depth RS measurements undertaken on plain samples.

The RS were measured in the notched peened samples along the notch bisector through two complementary experimental techniques: (i) μXRD and (ii) μHD, μSC.

The μXRD measurements are made employing a Bruker's D8 Discover XRD2 micro-diffractometer equipped with a General Area Diffraction Detection System (GADDS) and Hi-Star 2D area detector. Tube parameters of 40 kV/40 mA using Cu-K_α radiation at a detector distance of 30 cm covering approximately an area of 20° in 2θ and 20° in γ with 0.02° resolution. A focusing optic was used to achieve a beam diameter of 50 μm. The surface RS profile along the notch bisector was mapped through 11 measurements spaced 50μm apart starting from the notch tip. The Cu-K_α radiation due to its high penetration depth (≈ 40 μm) captures information about RSs throughout the entire surface layer modified by the peening treatment.

The μHD and μSC measurements are performed on specimens that had been previously polished using emery papers (grit ranging from 600 to 2400), abrasive aqueous suspensions (particle size ranging from 9 to 0.25 μm) and

0.05 μm colloidal silica solution. In this way, a surface layer of about 30 μm thickness is removed. As shown in [9], the removal of a thin surface layer does not significantly affect the RS distribution in the underlying material. A series of micro-holes (1μm in diameter and 1 μm deep) and micro-slots (6 μm long, 0.1 μm wide and 0.5 μm deep) are FIBed along the notch bisector using an FEI Nova Nanolab 600i. Davis LaVision DIC software is used to record the surface relaxations as the holes and the slots are milled. Further details on both measurements techniques can be found in [9].

3. Experimental results

3.1. Fatigue behavior

The results of the pulsating bending fatigue tests as well as the P50 fatigue lines are compared in Figs. 2a and 2b for unpeened and peened specimens, respectively. The parameters representing the fatigue curves corresponding to 50% of failure probability, according to Eqs. (1) and the results scatter, expressed by Eq. (2) are listed in Table 1.

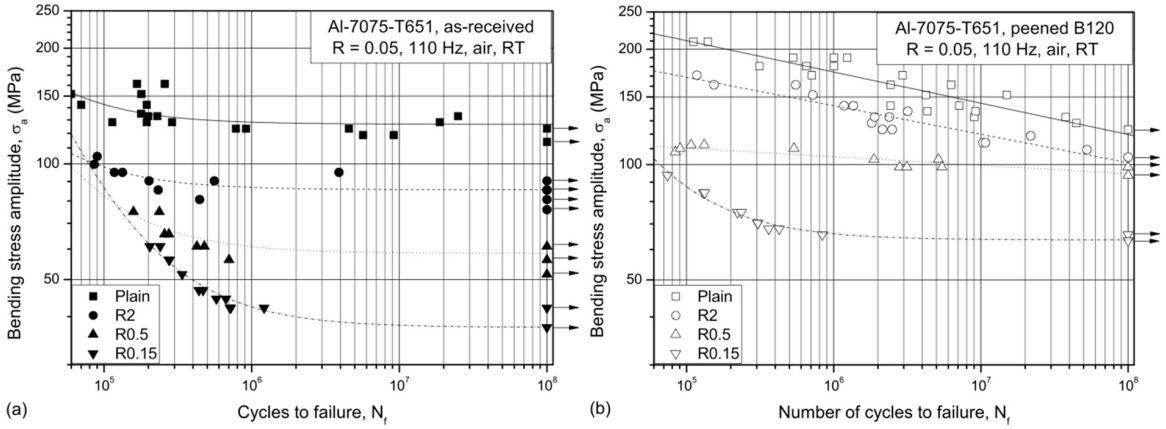

Fig. 2. S-N curves of the plain and notched specimens: (a) as-received, (b) peened specimens. Run-out tests are marked by arrows.

All the S-N of the as-received condition (fig. 2a) show a knee around 1×10^6 cycles. The stress raisers suppress the occurrence of failures at fatigue lives longer than 4×10^6 cycles in the as-received material and this phenomenon becomes more remarkable with increasing notch severity. Similar behavior can be observed for the peened samples carrying the very sharp notch. On the contrary, the S-N curves of the blunt and sharp-notched peened samples steadily decline with the fatigue life showing occurrence of failure throughout the explored life interval (fig. 2b).

Table 1. Principal results of the fatigue tests

Sample geometry	Condition	Wöhler curve				Gain (%)	
		Equation	k	σ_{0P50} (MPa)	$T\sigma$	@5×10^5 cycles	@5×10^7 cycles
Smooth	As-received	(1b)	1.60×10^6	127	1.24	42	0
	Peened B120	(1a)	12	540	1.18		
Blunt notched (R2)	As-received	(1b)	1.25×10^6	86	1.14	70	24
	Peened B120	(1a)	13	400	1.13		
Sharp notched (R0.5)	As-received	(1b)	2.41×10^6	58	1.17	68	64
	Peened B120	(1a)	45	140	1.08		
Very sharp notched (R0.15)	As-received	(1b)	4.91×10^6	38	1.13	44	69
	Peened B120	(1b)	2.41×10^6	64	1.07		

The peening treatment was effective in prolonging the fatigue life of the material as well as in reducing the large scatter in fatigue results displayed by the virgin material. The improvement depends on both the applied load and the notch severity. The increment in fatigue resistance due to shot peening steadily declines during fatigue life for smooth

and blunt-notched specimens, being more remarkable at high load levels corresponding to shorter fatigue lives, leading to higher values of the slope in the P_{50} fatigue line. While the plain fatigue performance at 10^8 cycles of the peened variants is comparable with that of the virgin material, an increment of about 20% in the fatigue resistance of blunt-notched specimens is still present in this fatigue regime. On the contrary, the increment due to shot peening is even higher for longer than for shorter fatigue in the case of sharp notches and for very sharp notches.

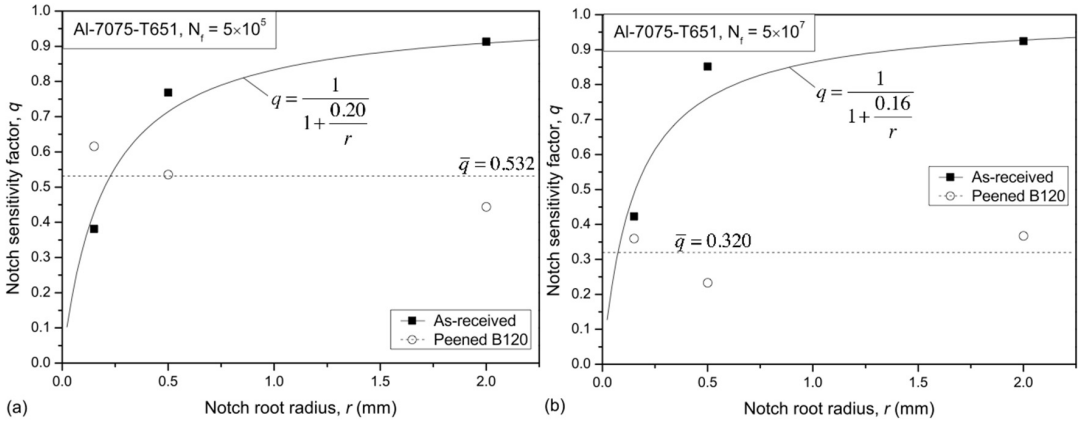

Fig. 3. Notch sensitivity factor dependence upon notch root radius for a fatigue live corresponding to (a) 5×10^5 and (b) 5×10^7 cycles.

Figures 3a and b illustrate the dependence of the notch sensitivity factor q on the notch root radius r for a fatigue life of 5×10^5 and 5×10^7, respectively. A remarkable reduction in notch sensitivity due to shot peening is evident, especially for the blunt notch R2. The dependence of the factor q upon the notch root radius for the unpeened samples is well represented by the Peterson equation:

$$q = \frac{1}{1+\frac{a}{r}} \tag{4}$$

where the material characteristic length a ranges between 0.16 and 0.20 mm. Conversely, for the peened variants the factor q seems to be not correlated to the notch root radius. An average value was found comprised between 0.53 and 0.32 at the lowest and highest fatigue life, respectively. Notably, for the very sharp-notched specimens, the q factor of the unpeened samples is lower at shorter and higher at longer fatigue life with respect to the peened samples. This confirms that the peening treatment on the most severe notches is more effective in the very high cycle fatigue regime.

3.2. Residual stress field around the notch

Figure 4a shows the average of the two μXRD measurements performed on opposite frontal faces as a function of the y coordinate (as defined in Fig. 1) aligned with the notch bisector and centred on the notch apex. It can be noted that the longitudinal RS component increases moving toward to the notch and that the stress concentration effect scales with the severity of the notch. The region affected by the notch spans over about 0.25 mm from the notch root.

Figure 4b illustrates the average of the two FIB/DIC measurements undertaken by the micro-hole and micro-slot techniques on the notched samples after removing the outer 30 μm thick surface layer from the frontal face. The FIB-DIC data match the trends in the μXRD measurements. The experimental results were used in [10,11] to reconstruct

the whole RS field acting on the notch symmetry plane. Specifically, the RS ahead of the notch was introduced into the finite element model through a temperature field, reproducing the effect of the peening treatment applied to the frontal and lateral surface as well as the boundary effects at the notch root edge.

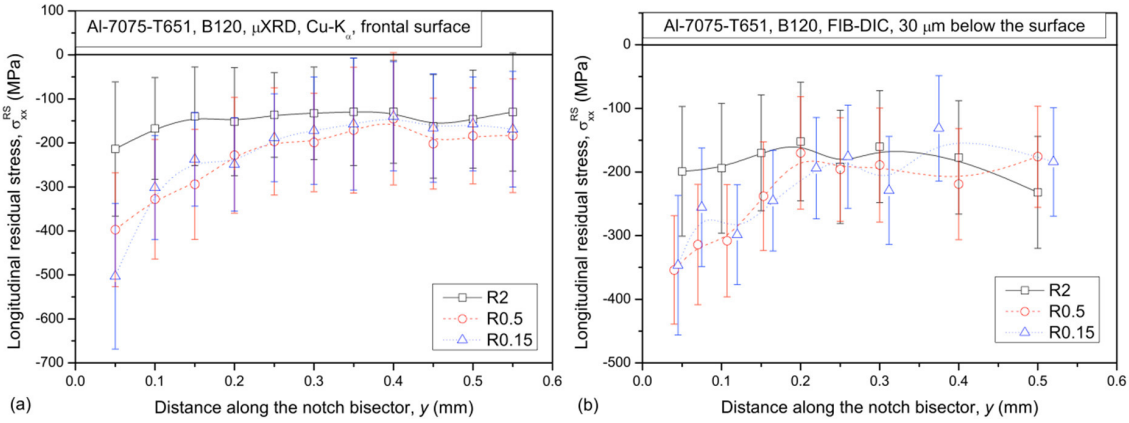

Fig. 4. Results of the measurements in terms of longitudinal RS distribution along the notch bisector. (a) Average of two measurements taken with the μXRD technique. (b) Average of the measurements taken with FIB-DIC μHD and μSC techniques.

Figure 5a-f illustrate the contour plot of the of the RS field as a function of the z (in-depth) and y (notch bisector) coordinates. Figures a, c, and e show the longitudinal RS component, while Figures b, d, and f display the transversal RS component. As pointed out by the experimental measures, a considerable concentration of the longitudinal RSs at the notch apex can be noted, especially in the sharpest notch.

4. Simulation of the fatigue behavior

The advantage of reconstructing the RS distribution around the notch is that the notch fatigue response can be predicted using a field approach instead of conventional fatigue criteria based on point stress values. Accordingly, the critical distance theory postulates that the notch fatigue response is governed by an effective stress, which is a function of the stress field in the neighborhoods of the notch root [12]. In [5] a line method was adopted, wherein the critical condition of a notched member is achieved when the effective stress, calculated by averaging an equivalent stress σ_{eq} along the notch bisector over a material characteristic length L, equals the plain fatigue strength f. This was assumed to be that of the unpeened material since the work hardening introduced by shot peening exerts a negligible influence on the fatigue resistance [3].

In the present work, the assumptions regarding the fatigue properties of the peened material are retained, whereas the theory of critical distance is applied in a different way. Instead of averaging the equivalent stress along the notch bisector lying on the frontal surface, the average is computed over a square area lying on the notch symmetry plane in order to capture the in-depth variation of the RS field:

$$\frac{1}{L^2}\int_0^L\int_0^L \sigma_{eq}\,dz\,dy = f \tag{5}$$

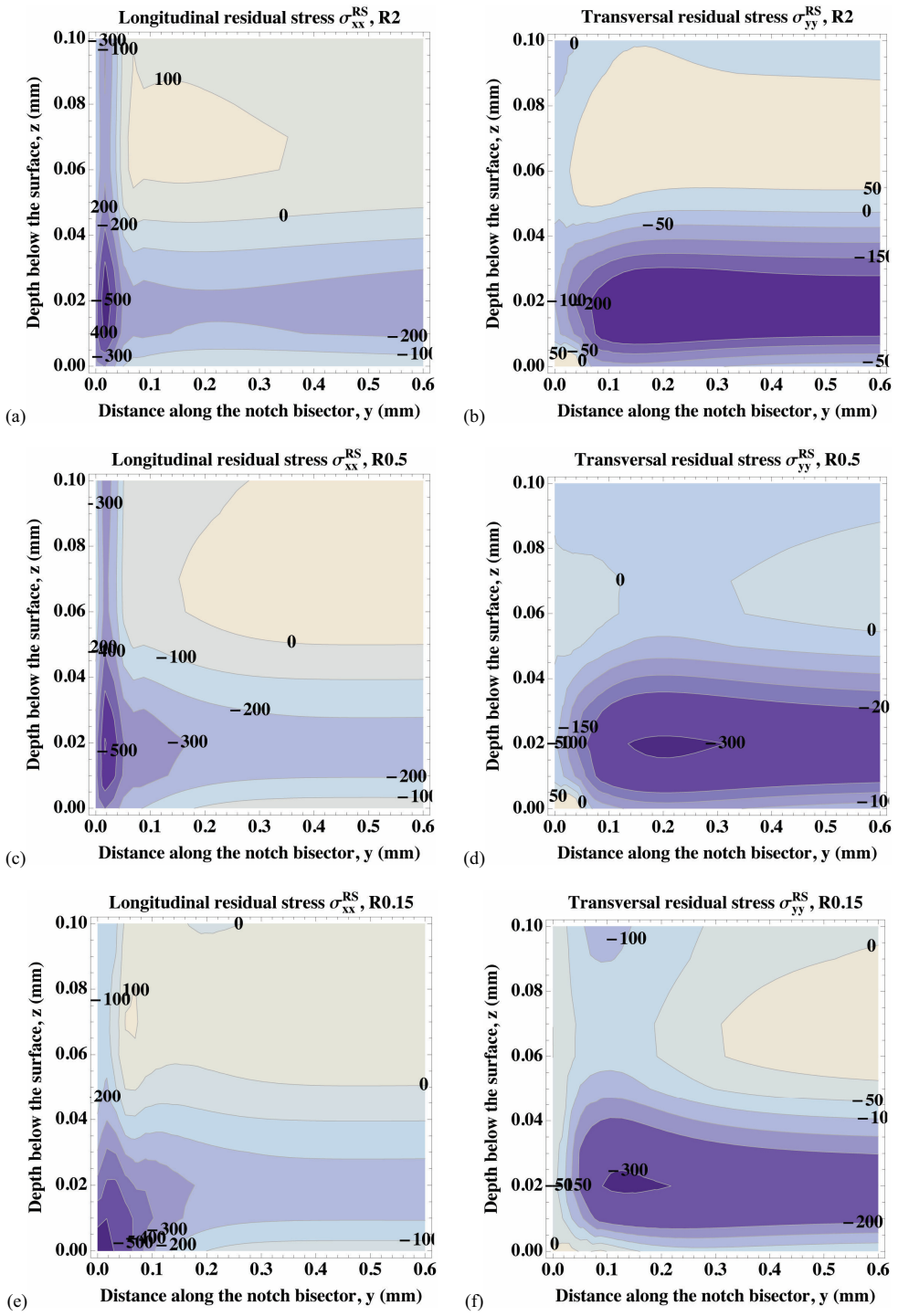

Fig. 5. Contour plots of the reconstructed RS field. (a),(c),(e) longitudinal, (b),(d), (f) transversal residual stress. (a),(b) blunt notch R2, (c),(d) sharp notch R0.5, (e),(f) very sharp notch R0.15.

The Crossland criterion was adopted for modelling the stress conditions at notches, since the loading is proportional and the criterion proved to successfully predict the fatigue response of peened components when the fatigue behavior is controlled by surface crack initiation [7]. Specifically, the Crossland criterion includes the Von Mises equivalent stress amplitude $\sigma_{VM,a}$ and the maximum hydrostatic pressure $p_{\max}$ in eqn.6. Under bending fatigue tests at nominal stress amplitude σ_a and load ratio R, $\sigma_{VM,a}$ and $p_{\max}$ are expressed in terms of the principal stresses' amplitude by eqn. 7.

$$\sigma_{eq} = \sigma_{VM,a} + \alpha_C \cdot p_{\max}; \quad f = \beta_C \tag{6}$$

$$\sigma_{VM,a} = \frac{1}{\sqrt{2}}\sqrt{\left(\sigma_{1,a}-\sigma_{2,a}\right)^2+\left(\sigma_{2,a}-\sigma_{3,a}\right)^2+\left(\sigma_{3,a}-\sigma_{1,a}\right)^2}$$
$$p_{\max} = \frac{\frac{2}{1-R}\left(\sigma_{1,a}+\sigma_{2,a}+\sigma_{3,a}\right)+\left(\sigma_1^{RS}+\sigma_2^{RS}+\sigma_3^{RS}\right)}{3} \tag{7}$$

The material properties α_C and β_C were determined in [7] at several fatigue lives from tension, torsion and in-phase combined tension–torsion tests. The critical distance L has been chosen equal to the El-Haddad distance [12], which is a function of both the range of the threshold stress intensity factor for crack propagation ($\Delta K_{th}\left(R=0\right)=2.4\,MPa\sqrt{m}$ [13]) and plain fatigue strength range at high number of cycles to failure ($\Delta f_0 = 254\,MPa$ [14]) determined at the same load ratio R:

$$L = \frac{1}{\pi}\left(\frac{\Delta K_{th}}{\Delta f_0}\right)^2 = 0.028\,mm \tag{8}$$

The comparison between the experimental data and the mean fatigue curves calculated according to the above procedure is shown in Fig. 6.

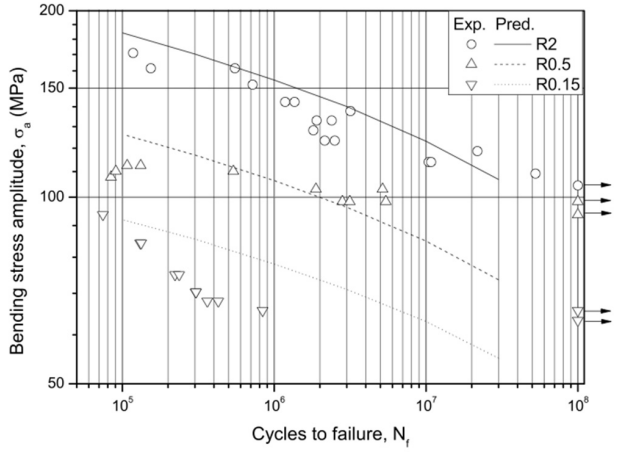

Fig. 6. Comparison between experimental data and calculated fatigue curves of the peened samples.

Despite a slight tendency of the Crossland criterion to overestimate the fatigue resistance in the medium-cycle regime, as already observed in [7], the proposed fatigue calculation method yields accurate estimations of the fatigue behavior of peened notched specimens. Accordingly, the relative error is lower than 15% within the entire explored fatigue life interval. In addition, it can be noted that the predicted fatigue curves for sharp and very sharp notches do not show the change in slope around 10^6 fatigue cycles displayed by the experimental data. This could be explained

by the fact that, since the predicted curve represents the condition of fatigue crack initiation, it is implicitly assumed that the fatigue life is preponderantly spent to nucleate a dominant crack. However, cracks nucleated at the notch tip due to the high stress concentration may become non-propagating far from the notch due to the steeply descending stress gradient and crack closure promoted by compressive RSs. This might explain the reason why the slope change in the fatigue line is more pronounced in sharper notches and in shot peened samples. This phenomenon will be matter of future investigations aimed at identifying the propagation threshold condition of fatigue cracks emanating from notches and embedded in a compressive RS field.

5. Conclusions

The notch fatigue strength of shot peened Al-7075-T651 alloy has been experimentally investigated exploring fatigue lives between 10^5 and 10^8. The fatigue improvement due to peening was discussed accounting for the residual stress effects. The residual stress field ahead of the notch root was numerically simulated starting from experimental values measured along the notch bisector with non-destructive and destructive techniques, namely micro-XRD and FIB-DIC micro-slot cutting and micro-hole drilling. The following conclusions can be drawn:

1. Shot peening strongly improve the fatigue behavior of Al-alloys even in the presence of geometrical discontinuities, resulting in greatly reduced notch sensitivity.
2. The sharp notches induce a remarkable residual stress concentration, whose entity scales with the notch severity.
3. The notch fatigue behavior can be satisfactorily simulated by the Crossland criterion incorporating residual stresses and combined with an area method based on the critical distance theory to account for the notch sensitivity.

References

[1] K.A. Soady, Life assessment methodologies incorporating shot peening process effects; mechanistic consideration of residual stresses and strain hardening. Part 1: the effect of shot peening on fatigue resistance. Mater. Sci. Technol. 29 (2013) 637– 651.
[2] K.A. Soady, B.G. Mellor, P.A.S Reed, Life assessment methodologies incorporating shot peening process effects; mechanistic consideration of residual stresses and strain hardening. Part 2: approaches to fatigue lifing after shot peening. Mater. Sci. Technol. 29 (2013) 652– 664.
[3] M. Benedetti, V. Fontanari, P. Scardi, C.L.A. Ricardo, M. Bandini, Reverse bending fatigue of shot peened 7075-T651 aluminium alloy: The role of residual stress relaxation. Int J Fatigue. 31 (2009) 1225-1236.
[4] M. Benedetti, V. Fontanari, B.D. Monelli, Numerical simulation of residual stress relaxation in shot peened high-strength aluminium alloys under reverse bending fatigue. ASME J Eng Mater Technol. 132 (2010) 011012.
[5] M. Benedetti, V. Fontanari, C. Santus, M. Bandini, Notch fatigue behaviour of shot peened high-strength aluminium alloys: experiments and predictions using a critical distance method. Int J Fatigue. 32 (2010) 1600–1611.
[6] M. Benedetti, V. Fontanari, M. Bandini, A simplified and fast method to predict plain and notch fatigue of shot peened high-strength aluminium alloys under reverse bending. Surface&Coatings Technology. 243 (2014) 2–9.
[7] M. Benedetti, V. Fontanari, M. Bandini, D. Taylor, Multiaxial fatigue resistance of shot peened high-strength aluminum alloys. Int J Fatigue. 61 (2014) 271–282.
[8] M. Benedetti, V. Fontanari, M. Bandini. E. Savio, High- and very high-cycle plain fatigue resistance of shot peened high-strength aluminum alloys: The role of surface morphology. Int. J. Fatigue. 70 (2015) 451-462.
[9] B. Winiarski, M. Benedetti, V. Fontanari, M. Allahkarami, J. C. Hanan, G.S. Schajer, P.J. Withers, Comparative Analysis of Shot-Peened Residual Stresses Using Micro-Hole Drilling, Micro-Slot Cutting, X-Ray Diffraction Methods and Finite- Element Modelling. Proceedings of the SEM 2015 Annual Conference & Exposition on Experimental and Applied Mechanics, Costa Mesa, CA USA, 2015.
[10] M. Benedetti, V. Fontanari, M. Allahkarami, J. C. Hanan, B. Winiarski, P.J. Withers, Modelling the Residual Stress Field Ahead of the Notch Root in Shot Peened V- Notched Samples. Proceedings of the SEM 2015 Annual Conference & Exposition on Experimental and Applied Mechanics, Costa Mesa, CA USA, 2015.
[11] M. Benedetti, V. Fontanari, B. Winiarski, P.J. Withers, M. Allahkarami, J.C. Hanan, Residual stresses in shot peened notched specimens. Part II: Modelling by experimental measurements and finite element analysis. Manuscript in preparation for publication in Experimental Mechanics, 2015.
[12] L. Susmel, The theory of critical distances: a review of its applications in fatigue. Eng Fract Mech. 75 (2008) 1706–24.
[13] A.H. Noroozi, G. Glinka, S. Lambert, Prediction of fatigue crack growth under constant amplitude loading and a single overload based on elasto-plastic crack tip stresses and strains. Eng Fract Mech. 75 (2008) 188–206.
[14] M. Benedetti, V. Fontanari, B.D. Monelli, Plain fatigue resistance of shot peened high strength aluminium alloys: effect of loading ratio. Procedia Eng. 2 (2010) 397–406.